Plasmonic Dual D-shaped PCF Sensor for Low Refractive Index Applications

Yusuf Gamal[1,3], B. M. Younis[2,3], Mohamed Farhat O. Hameed[3*], and S. S. A. Obayya[3*]

[1]Engineering Application of Laser Department, National Institute of Laser Enhanced Science (NILES), Cairo University, Egypt.

[2]Electronics and Communications Engineering Department, Misr Higher Institute for Engineering and Technology (MET), Mansoura, Egypt

[3]Center for Photonics and Smart Materials, Zewail City of Science and Technology, October Gardens, 6th of October City, Giza 12578, Egypt. E-mail: mfarahat@zewailcity.edu.eg, sobayya@zewailcity.edu.eg

Abstract— **Dual D-shaped (DD-shaped) plasmonic photonic crystal fiber (PCF) for refractive index sensing is designed and analyzed. In the proposed design, two gold nano-rods are attached to the two etched surfaces of the PCF to enhance the sensing characteristics. The surface plasmon (SP) modes excited at the metal/dielectric interfaces are strongly coupled to the PCF core mode. Therefore, high refractive index (RI) sensitivity of 19100 nm/RIU is achieved. Such a sensor can be employed in environmental monitoring and food safety applications.**

***Index Terms*— Photonic crystal fibers, Refractive index sensor, surface plasmon, Environmental monitoring.**

Design and study of compact and integrated photonic devices is the most recent development in photonics science. Coupling between surface plasmon modes (SPMs) excited at the metal/dielectric interface and the core-guided modes is the main concept of the surface plasmon resonance (SPR) sensing mechanism[1]. This coupling occurs when the real part of the effective indices of a SPM and the core mode are equal. In this case, maximum power transfer from core mode to the SPM is achieved. This resonance occurs at a specified wavelength with a certain RI of the surrounding medium (analyte). When the analyte RI is changed, a shift in the resonance wavelength is induced. Thus, the sensitivity is detected. SPR technique has been applied to many types of optical devices including filters[2], optical absorbers[3] and optical instruments[4].

Among the most often utilized platforms in sensing applications, PCFs arouse great importance in sensing[5,6,7], salinity detection[8], and food safety and environmental monitoring [9]. In this context, a self-calibration plasmonic PCF biosensor has been analyzed in[10] with sensitivities of 10000 nm/RIU and 6700 nm/RIU for the x- and y-polarized core modes, respectively. Further, a low refractive index sensor of concave-shaped PCF combined was designed with square-channel using lossy material indium tin oxide (ITO) [11]. Such a RI sensor[11] achieves sensitivities of 1700–10700 nm/RIU with a dynamic RI range from 1.19 to 1.29. Furthermore, liu *et al.* [12] introduced a low RI sensor based on SPR mechanism with gold nanowires with sensitivity of 2350 nm/RIU. In addition, Hasan *et al.* [13] proposed a PCF biosensor based on a two-layer circular lattice that achieves sensitivity of 2200 nm/RIU. Moreover, An *et al.* introduced a quasi-D-shaped PCF sensor with a sensitivity of 3877 nm/RIU through RI range from 1.33 to 1.42 [14]. Furthermore, Rifaat *et al.*[15] presented a SPR-PCF sensor with sensitivity of 11000 nm/RIU for a wide range of analyte RI where irregular air-hole diameters have been used in the first ring.

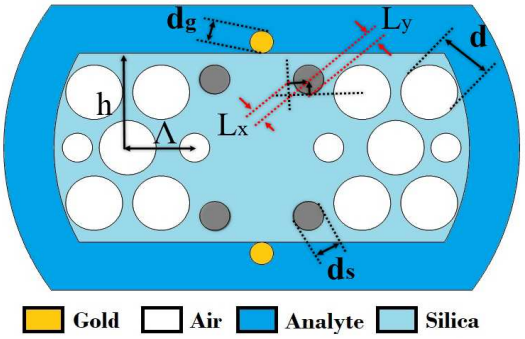

Fig. 1 The cross sections of dual D-shaped PCF SPR multifunctional biosensor.

Figure 1 depicts the proposed structure using three successive rings of air holes arranged in a triangular lattice with a hole pitch Λ and silica (SiO_2) background material. The first ring of air holes have diameter d_s, while the second and third rings have a diameter d. In addition, the two surfaces of the PCF structure are etched at a distance h from the horizontal line passing through the core center as shown in Fig. 1. To excite SPM, two gold nano-rods with diameter d_g are attached vertically at the two etched surfaces. In addition, four holes (in gray color) in the first ring are shifted horizontally with l_x and l_y distances as depicted in Fig. 1. The frequency-dependent gold permittivity is taken from the model of Johnson and Christy [16,17]. Additionally, silica RI is determined by the wavelength dependent Sellmeier equation[1,2]. In this investigation, COMSOL Multiphysics software package [18] based on the well-known full vectorial finite element method (FVFEM)[19] is utilized to study and analyze the proposed PCF structure. The PCF structure is discretized into small triangular elements with a minimum element size of 3×10^{-4} μm. Moreover, perfect matched layer (PML) [20] absorbing boundary conditions is employed to truncate

the simulation domain from all transverse directions and calculate the confinement losses of the studied modes.

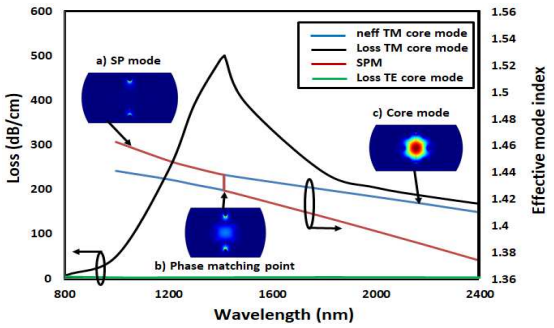

Fig. 2. Dispersion of the quasi TM core modes and SPP mode and variation of the loss spectra of quasi TM, quasi TE and SPP modes with the wavelengths.

The dispersion characteristics of the core mode and SPM supported by the DD-shaped PCF structure are depicted in Fig. 2. The real parts of the effective indices of the quasi TM core mode and SPM are shown as blue and red lines, respectively. The n_{eff} of the quasi TM core mode and SPM decrease with increasing the wavelength. Moreover, the attenuation loss of the TM core mode has a loss peak at the phase matching wavelength as shown in Fig. 2. The insets (a), (b) and (c) depict the electric field profiles of the SPM (at λ=1000 nm), the core mode at the phase matching point (at λ = 1417 nm) and quasi TM core mode (at λ=1000 nm), respectively. At the resonance wavelength, there is a strong coupling between the SPM and the quasi TM core mode as both have approximately the same electric field distribution with nearly identical effective indices. However, the loss of the quasi TE mode (green line) is very small throughout the whole considered wavelength range as may be seen in Fig. 2.

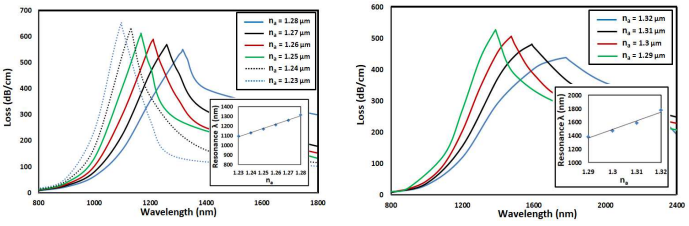

(a) (b)

Fig. 3 Variation of the attenuation loss spectra with the wavelength at (a) RI range from 1.23 to 1.28, and (b) RI range from 1.29 to 1.32.

It may be seen from Figs. 3 (a) and (b) that increasing the analyte RI moves the loss peaks to longer wavelengths. Further, high RI sensitivity of 19100 nm/RIU is obtained with a resolution of 5.2×10^{-6} RIU. Due to high sensitivity throughout wide low refractive indices (1.23 – 1.32), the proposed sensor is a promising candidate especially in environmental monitoring and food safety applications[9, 11, 12]. Moreover, As may be seen from the two insets in Figs 3(a) and (b), the suggested sensor has a linear-like behavior over the RI range from 1.23 to 1.32.

Finally, a highly sensitive D-shaped PCF low refractive indices sensor that works along wide RI range (1.23-1.32) is reported. The proposed sensor achieves sensitivity and resolution of 19100 nm/RIU and 5.2×10^{-6} RIU, respectively, with high linearity behavior.

ACKNOWLEDGMENT

The authors acknowledge the financial support by Science, Technology & Innovation Funding Authority (STIFA) at Egypt, project ID (45702).

REFERENCES

1. Akowuah, E. K. *et al.* Numerical analysis of a photonic crystal fiber for biosensing applications. *IEEE J. Quantum Electron.* **48**, 1403–1410 (2012).
2. Gamal, Y. *et al.* Highly efficient modified dual D-shaped PCF polarization filter. *Opt. Fiber Technol.* **62**, 102459 (2021).
3. Wang, Y. *et al.* Triple-band perfect metamaterial absorber with good operating angle polarization tolerance based on split ring arrays. *Results Phys.* **16**, 102951 (2020).
4. Wang, X. *et al.* Surface plasmons and SERS application of Au nanodisk array and Au thin film composite structure. *Opt. Quantum Electron.* **52**, 1–11 (2020).
5. Gamal, Y. *et al.* Highly Sensitive Multi-Functional Plasmonic Biosensor Based on Dual Core Photonic Crystal Fiber. *IEEE Sens. J.* (2022).
6. Gamal, Y. *et al.* Highly Sensitive Plasmonic PCF Biosensor. in *2021 International Applied Computational Electromagnetics Society Symposium (ACES)* 1–2 (IEEE, 2021).
7. Azzam, S. I., Hameed, M. F. O., Shehata, R. E. A., Heikal, A. M. & Obayya, S. S. A. Multichannel photonic crystal fiber surface plasmon resonance based sensor. *Opt. Quantum Electron.* **48**, 142 (2016).
8. Adamo, F., Attivissimo, F., Carducci, C. G. C. & Lanzolla, A. M. L. A smart sensor network for sea water quality monitoring. *IEEE Sens. J.* **15**, 2514–2522 (2014).
9. Haque, E. *et al.* Highly sensitive dual-core PCF based plasmonic refractive index sensor for low refractive index detection. *IEEE Photonics J.* **11**, 1–9 (2019).
10. Hameed, M. F. O., Alrayk, Y. K. A. & Obayya, S. S. A. Self-calibration highly sensitive photonic crystal fiber biosensor. *IEEE Photonics J.* **8**, 1–12 (2016).
11. Yang, Z., Xia, L., Li, C., Chen, X. & Liu, D. A surface plasmon resonance sensor based on concave-shaped photonic crystal fiber for low refractive index detection. *Opt. Commun.* **430**, 195–203 (2019).
12. Liu, C. *et al.* Analysis of a surface plasmon resonance probe based on photonic crystal fibers for low refractive index detection. *Plasmonics* **13**, 779–784 (2018).
13. Hasan, M., Akter, S., Rifat, A. A., Rana, S. & Ali, S. A highly sensitive gold-coated photonic crystal fiber biosensor based on surface plasmon resonance. in *Photonics* vol. 4 18 (Multidisciplinary Digital Publishing Institute, 2017).
14. An, G., Li, S., Wang, H., Zhang, X. & Yan, X. Quasi-D-shaped optical fiber plasmonic refractive index sensor. *J. Opt.* **20**, 35403 (2018).
15. Rifat, A. A. *et al.* Highly sensitive selectively coated photonic crystal fiber-based plasmonic sensor. *Opt. Lett.* **43**, 891–894 (2018).
16. Johnson, P. B. & Christy, R.-Wjp. Optical constants of the noble metals. *Phys. Rev. B* **6**, 4370 (1972).
17. Hameed, M. F. O. & Obayya, S. *Computational photonic sensors*. (Springer, 2019).
18. COMSOL 5.1. Multiphysics software. https://www.comsol.com (2020).
19. Obayya, S. S. A., Rahman, B. M. A., Grattan, K. T. V & El-Mikati, H. A. Full vectorial finite-element-based imaginary distance beam propagation solution of complex modes in optical waveguides. *J. Light. Technol.* **20**, 1054 (2002).
20. Koshiba, M. & Tsuji, Y. Curvilinear hybrid edge/nodal elements with triangular shape for guided-wave problems. *J. Light. Technol.* **18**, 737–743 (2000).